A change from stepwise to concerted mechanism in the acid–catalysed benzidine rearrangement: A theoretical study

ARTICLE *in* TETRAHEDRON · MARCH 2012

Impact Factor: 2.64 · DOI: 10.1016/j.tet.2012.01.014

3 AUTHORS, INCLUDING:

Giovanni Ghigo
Università degli Studi di Torino
54 PUBLICATIONS **1,480** CITATIONS
SEE PROFILE

Glauco Tonachini
Università degli Studi di Torino
96 PUBLICATIONS **1,344** CITATIONS
SEE PROFILE

Tetrahedron 68 (2012) 2161–2165

Contents lists available at SciVerse ScienceDirect

Tetrahedron

journal homepage: www.elsevier.com/locate/tet

A change from stepwise to concerted mechanism in the acid-catalysed benzidine rearrangement: a theoretical study

Giovanni Ghigo *, Andrea Maranzana, Glauco Tonachini

Dipartimento di Chimica Generale e Chimica Organica, C.so M. d'Azeglio 48, I-10125 Torino, Italy

ARTICLE INFO

Article history:
Received 20 October 2011
Received in revised form 22 December 2011
Accepted 9 January 2012
Available online 16 January 2012

Keywords:
Benzidine rearrangement
DFT
Reaction

ABSTRACT

The *monoprotonated* mechanism of the benzidine acid-catalysed rearrangement of hydrazobenzene (corresponding to a second order kinetics) is studied and compared with the *diprotonated* mechanism (corresponding to a third order reaction and previously studied). The nature of the two mechanisms is found to be completely different: a concerted closed-shell sigmatropic shift in the *monoprotonated*, a stepwise radical cation recoupling in the *diprotonated*. The activation energies, combined with the energetics of the protonation equilibria, are also very different: 35 kcal mol^{-1} for the former and 26 kcal mol^{-1} for the latter (in good agreement with the experimental data). These values make the third order *diprotonated* mechanism favoured with respect to the second order *monoprotonated* mechanism for the rearrangement of hydrazobenzene, as found at typical experimental acid concentrations.

1. Introduction

The acid-catalysed benzidine rearrangement consists in the intramolecular conversion of aromatic hydrazo compounds in diaminobiphenyls (4,4′ or 2,4′ or 2,2′) and semidines (2 or 4), depending on the substrate.[1] At first glance these conversions seem to be simple sigmatropic shifts but this was found to be inadequate to explain all experimental findings. In fact, despite the large amount of experimental work and the mechanisms proposed, this rearrangement has not been fully described yet.[2] Therefore, two years ago[3] we undertook a theoretical study on this reaction and we succeeded, we believe, to clarify the mechanism, at least for the parent reaction, the hydrazobenzene rearrangement (Scheme 1, **1**).[4]

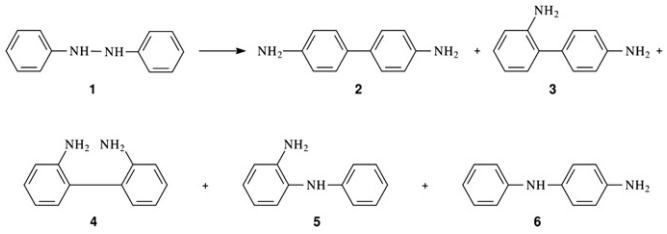

Scheme 1. The benzidine rearrangement of hydrazobenzene.

In our model, where both the experimental yields of the main products (Schemes 1–3) and the kinetic isotope effects are well reproduced, the reaction has been found to take place through a multi-step mechanism where π-complexes with a dication diradical character similar to those proposed by Dewar[5] play a major role. We report that some elements of the mechanism were also proposed in a theoretical work by Yamabe et al.[6]

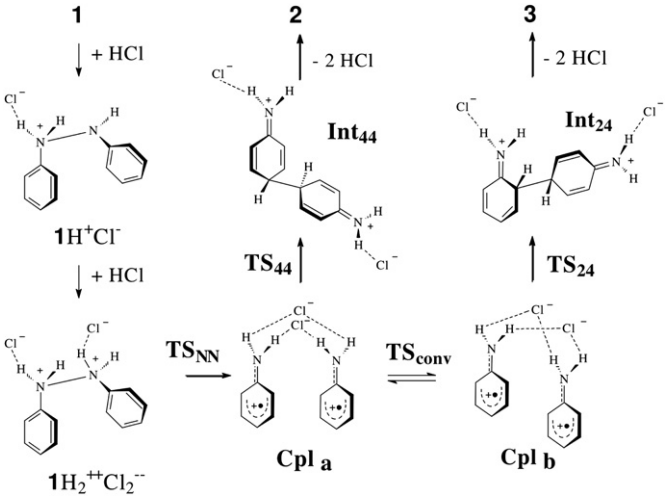

Scheme 2. Pathways in the third order *diprotonated* benzidine rearrangement.

* Corresponding author. E-mail address: giovanni.ghigo@unito.it (G. Ghigo).

0040-4020/$ – see front matter © 2012 Elsevier Ltd. All rights reserved.
doi:10.1016/j.tet.2012.01.014

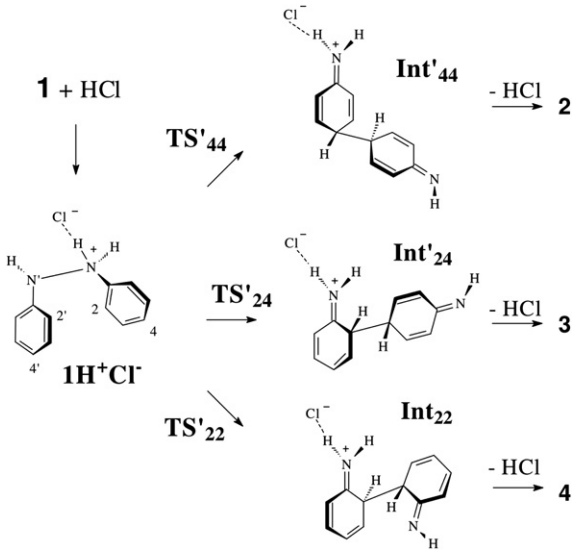

Scheme 3. Pathways in the second order *monoprotonated* benzidine rearrangement.

One of the key points of this reaction is the dependence of its rate on the acid concentration. The kinetics are first order in the substrate concentration [**1**] but can be first order in [H^+] (second order on the whole) or second order in [H^+] (third order on the whole). In fact, depending on the nature of the substrate and on the acid concentration, second or third order kinetics or even intermediate kinetics have been observed.[1,2] This dichotomy is due to the occurrence of two competing mechanisms[7]: the first one is a second order '*monoprotonated*' mechanism with rate constant k_m; the second one is a third order '*diprotonated*' mechanism with rate constant k_d:

$$v = k_m[\mathbf{1}]\left[H^+\right] + k_d[\mathbf{1}]\left[H^+\right]^2 \quad (1)$$

The kinetics for the hydrazobenzene rearrangement were definitively established in 1950 when it was found to be second order in [H^+].[8] Later on,[9] this was confirmed and the k_d estimated. The k_m value, included in the model, was found to be substantially null at the experimental conditions. For this reason our first study[4] was focused on the *diprotonated* mechanism only and no attempt to explore the *monoprotonated* mechanism was undertaken. However, three questions remain unanswered: (1) what is the mechanism of the *monoprotonated* rearrangement for the parent reaction; (2) why this mechanism is not competitive; (3) which conditions might make this to prevail. In this work we try to answer these questions.

2. Results and discussion

The present section is structured in three parts. First, we shortly re-examined the *diprotonated* mechanism reaction in aqueous acid solution. Then we present the results of the theoretical study of the mechanism of the *monoprotonated* mechanism. Finally, a comparison of the two mechanisms is drawn and possible answers to the above questions are offered.

2.1. The diprotonated mechanism

This case has already been fully explored in the previous work,[4] so we will not describe it at the length. In the present study, only the most relevant structures, leading to the main products **2** and **3**, have been reconsidered (Scheme 1). Their electronic energies have been refined by single-point calculations with the larger basis set (this was not done in the previous work[4]) and combined with the thermal corrections recalculated at 273.15 K (Table 1). The dissociation limit corresponds to the energy of two aniline radical cation chlorides. The third order rearrangement has been found to take place through a multi-step mechanism. The diprotonated reactant (**1**$H_2^{++}Cl_2^{--}$) undergoes a homolytic breaking of the NN bond (TS_{NN}) yielding a complex (Cpl_a) with dication diradical character and similar to that ones proposed by Dewar. This complex can form a bond between the 4 and 4′ carbon atoms through a radical coupling (TS_{44}) yielding the intermediate Int_{44} whose deprotonation leads to the main rearrangement product (*p*-benzidine, **2**).

Table 1
Relative energies (in kcal mol^{-1}) for the *diprotonated* mechanism in water

	ΔE(0 K)[a]	ΔG(273 K)[b]	ΔG(298 K)[c]
1$H_2^{++}Cl_2^{--}$	0.0	0.0	0.0
TS_{NN}	11.6	12.6	12.7
Cpl_a	−0.5	−0.7	−0.8
TS_{44}	10.2	11.1	11.2
Int_{44}	−4.3	−3.7	−3.7
TS_{CONV}	7.2	7.5	7.5
Cpl_b	4.9	5.1	5.0
TS_{24}	11.2	11.8	11.8
Int_{24}	−5.1	−5.3	−5.3
Dissociation limit	17.5	5.4	3.4

[a] Electronic energy+ZPE.
[b] Free energy at 273 K.
[c] Free energy at 298 K.

As an alternative, Cpl_a can reversibly transform in a second dication diradical complex (Cpl_b) from which the precursor (Int_{24}) of the minor product (diphenyline **3**) can be obtained through TS_{24}. As can be seen comparing Table 1 with Table 1 in Ref. 4, the numerical differences are not significant. The relative yields, calculated with the new data at 0 °C for products **2** and **3** are 78 and 22%, and differ to some extent from the previous data calculated at 298 K (63 and 37%)[4] and from the experimental values (ca. 70 and 30%).[1,10] The free energy barrier for the first step (TS_{NN}) is used for the forthcoming comparison between the two mechanisms.

2.2. The monoprotonated mechanism

The theoretical study indicates that the monoprotonated hydrazobenzene chloride undergoes three concerted sigmatropic rearrangements leading to different intermediates (Scheme 3). These intermediates, after deprotonation and proton transfer, are converted into the final products. Relative energies are collected in Table 2. Because the experiments were performed in an aqueous environment both at 25 and 0 °C, the free energy values are reported at these two temperatures. The dissociation limit corresponds to the energy of an iminocyclohexadienyl cation chloride and aniline (Chart 1). The easier rearrangement leads to the intermediate Int'_{44} precursor of the main product **2** through the concerted transition structure TS'_{44} ($r_{NN'}$=3.850 Å; $r_{C4C4'}$=2.500 Å;

Table 2
Relative energies (in kcal mol^{-1}) for the *monoprotonated* mechanism in water

	ΔE(0 K)[a]	ΔG(273 K)[b]	ΔG(298 K)[c]
1H^+Cl^-	0.0	0.0	0.0
TS'_{44}	29.9	31.6	31.8
Int'_{44}	9.5	9.8	8.2
TS'_{22}	30.0	31.8	31.9
Int'_{22}	13.9	15.7	15.8
TS'_{24}	33.2	34.4	35.3
Int'_{24}	13.0	14.4	14.5
Dissociation limit	41.9	30.7	29.7

[a] Electronic energy+ZPE.
[b] Free energy at 273 K.
[c] Free energy at 298 K.

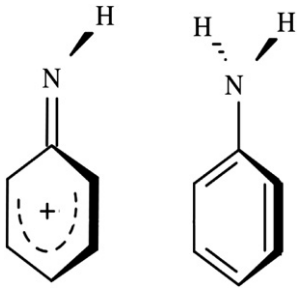

Chart 1. Dissociation fragments for the second order *monoprotonated* benzidine rearrangement.

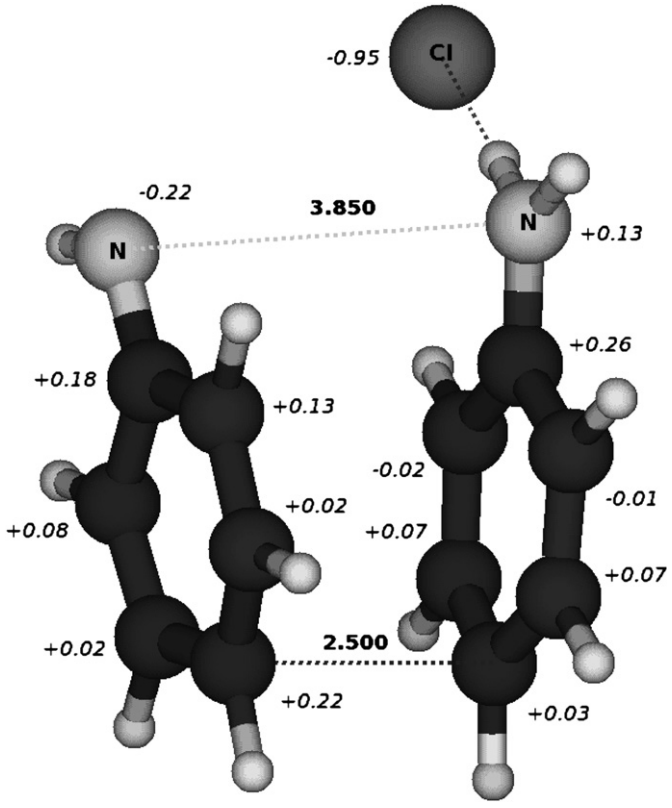

Fig. 1. The transition structure TS'_{44} for concerted rearrangement to intermediate Int'_{44}. Distances in Å. Group charges in italics.

Fig. 1). Its energy is quite high (ca. 30 kcal mol^{-1}). The positive group charge, initially mainly localized on the NH_2 group (q=+0.5) in $\mathbf{1}H^+Cl^-$, (Fig. SI-A in Supplementary data) is spread all over the structure in TS'_{44}. In Int'_{44} (Fig. SI-B) the positive charge is delocalized on the aniline moiety. During the rearrangement, the positive charge partially moves from the NH_2 group in $\mathbf{1}H^+Cl^-$ to the iminocyclohexadienyl moiety in TS'_{44} then to the aniline moves from the NH_2 group in $\mathbf{1}H^+Cl^-$ to the iminocyclohexadienyl moiety in TS'_{44} then to the aniline moiety in Int'_{44}. Another two concerted rearrangements have been found: one leads to Int'_{22} (Fig. SI-D) precursor of product **4** through TS'_{22} ($r_{NN'}$=3.976 Å; $r_{C2C2'}$=3.006 Å, Fig. SI-C) whose energy is very close to the former; the second leads to intermediate Int'_{24}, (Fig. SI-F) precursor of product **3** through TS'_{24} (r_{NN}=3.727 Å; r_{C2C4}=2.500 Å, Fig. SI-E) located 3 kcal mol^{-1} above the previous ones.

Pathways leading to intermediates Int'_{2N} (precursor of product **5**) and Int'_{4N} (precursor of product **6**) were not found. Partial transfers of the positive charge are also observed in these pathways. All these pathways present high energy barriers, so the *monoprotonated* mechanism is expected to be very slow. This result is coherent with the observed null k_m and will be also discussed later.

2.3. Comparison between the two mechanisms

The nature of the two mechanisms is completely different: the third order *diprotonated* is a stepwise radical cation recoupling while the second order *monoprotonated* is a concerted closed-shell sigmatropic shift. The latter is not stepwise because a stable complex between the dissociation fragments (aniline and iminocyclohexadienyl cation chloride, Chart 1) is absent. This complex, to exist, should form through non-covalent but strong enough interactions between the two facing fragments, where one of them (aniline) is a low polarity neutral molecule. However, this interaction cannot compensate for the stronger covalent N–N bond found in the reactant, whose energy corresponds to the dissociation limit (Table 2, ΔE(0 K)=42 kcal mol^{-1}, nor for the C–C bond found in the intermediates (ΔE(0 K)=28 kcal mol^{-1}. Therefore, as the N–N bond cleaves, the new C–C forms in the same step. In the *diprotonated* mechanism the dissociation level (Table 1) is more than 20 kcal mol^{-1} lower and the nature of the complexes (Cpl_a and Cpl_b) is different because, along with the van der Waals interactions, they present also a covalent character due to the partial radical coupling (see Ref. 4 for more details). Both factors guarantee the existence of these complexes and lead to a stepwise mechanism. The activation energies are also very different: less than 13 kcal mol^{-1} for the *diprotonated* mechanism and more than 30 for the *monoprotonated.* This direct comparison of the barriers involved is, however, not correct because the *diprotonated* mechanism requires, obviously, a second protonation. In fact, the whole reaction scheme for the acid-catalysed rearrangement is described by the following equations[8]:

$$\mathbf{1} + H^+ \underset{K'_a}{\rightleftarrows} \mathbf{1}H^+ \tag{2}$$

$$\mathbf{1}H^+ \xrightarrow{k'} Int' \tag{3}$$

$$\mathbf{1}H^+ + H^+ \underset{K''_a}{\rightleftarrows} \mathbf{1}H_2^{++} \tag{4}$$

$$\mathbf{1}H_2^{++} \xrightarrow{k''} \mathbf{Int} \tag{5}$$

k' and k'' are the rearrangement rate constants starting, respectively, from $\mathbf{1}H^+$ and $\mathbf{1}H_2^{++}$ and they can be calculated from the free energy barriers presented in this work. K_a' and K_a'' are the dissociation acid constants of the monoprotonated ($\mathbf{1}H^+$) and the diprotonated ($\mathbf{1}H_2^{++}$) hydrazobenzenes and they are taken from Ref. 2a.[11] Their values are 5 M and 10^6–10^7 M, respectively. From the reciprocal of their values (for K_a'' we use a mean value of 5×10^6 M) we can calculate the reaction free energies for the equilibria as shown in Eqs. 2 ($\Delta G'$) and 4 ($\Delta G''$). These are 2.6 kcal mol^{-1} and 10.1 kcal mol^{-1} at 0 °C and 2.8 kcal mol^{-1} and 11.0 kcal mol^{-1} at room temperature, respectively. From Eqs. 1–5 we obtain:

$$k_m = \frac{k'}{K'_a} \tag{6a}$$

$$k_d = \frac{k''}{K'_a K''_a} \tag{6b}$$

These equations correspond, in terms of activation free energies and making reference to the rate determining step of each mechanism, to:

$$\Delta G^{\ddagger}_{m} = \Delta G(TS'_{44}) + \Delta G' \quad (7a)$$

$$\Delta G^{\ddagger}_{d} = \Delta G(TS_{NN}) + \Delta G' + \Delta G'' \quad (7b)$$

For the *monoprotonated* mechanism we obtain, respectively, at 0 °C and at room temperatures, $\Delta G^{\ddagger}_{m}$=34.2 and 34.6 kcal mol^{-1}. For the *diprotonated* mechanism we obtain $\Delta G^{\ddagger}_{d}$=25.3 and 26.5 kcal mol^{-1}. The latter figures can be compared[12] with the experimental values[13] of 23–25 kcal mol^{-1}. Clearly the *diprotonated* mechanism is expected to be the faster. However, the comparison between the two mechanisms requires to include also the acid concentration. In the typical experimental condition this spans from 10^{-3} to 1 M. For these values we can estimate the following rate ratios[14] $k_d[H^+]^2/k_m[H^+]$: 10^4 and 10^7 at 0 °C or 10^3 and 10^6 at room temperature. It is evident that the contribution of the *monoprotonated* mechanism to the acid-catalysed rearrangement of hydrazobenzene is negligible. This mechanism might play a role only at very low acid concentration. At room temperature, the condition $k_d[H^+]^2=k_m[H^+]$ entails an acid concentration of 10^{-6} M. Clearly, the reaction rate under these conditions is expected to be negligible (ca. 10^{-10} M^{-2} s^{-1}).

The presence of a positive charge on the structures should make the reaction sensitive to the presence (and position) of substituents with an electron donating effect. The effect could also be different for the two mechanisms, making possible a contribution of the second order *monoprotonated* mechanism. This is, indeed, what is experimentally found for hydrazobenzenes that are methyl and methoxy substituted.[1,2,7,9] A possible explanation can be found by inspection of the charge distributions in the charged fragments at the dissociation limits (Chart 2). The charged fragment of the *monoprotonated* mechanism (A), shows partial positive charges mainly on the aromatic ring By contrast, the radical cation fragment for the *diprotonated* mechanism (B) shows, in the same positions, significantly lower partial positive charges. Clearly this should make the *monoprotonated* mechanism more sensitive to the electron donor substituents than the *diprotonated*.

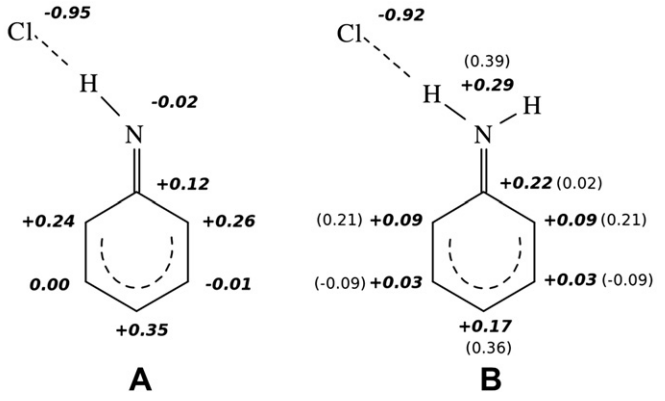

Chart 2. Charged dissociation fragments for the benzidine rearrangement. A: iminocyclohexadienylium chloride (*monoprotonated* mechanism); B: radical anilinium chloride (*diprotonated* mechanism). Group charges in italics. Group spin densities in parenthesis.

3. Conclusion

In the acid-catalysed benzidine rearrangement of hydrazobenzene, the second order reaction, corresponding to a *monoprotonated* mechanism, takes place through concerted transition structures without the interposition of any complex. By contrast, the third order reaction (corresponding to a *diprotonated* mechanism) was found[4] to take place through radical cations recoupling with the interposition of diradical dication Dewar's complexes. Our computations show that, though both mechanisms can concur to the rearrangement, due to the very different energy barriers calculated for the title system, only the third order mechanism (the *diprotonated*) has a real role in this reaction (as experimentally found). However, by inspection of the electronic structure of the fragments, we can deduce that the presence of electron donor substituents in positions 2 or 4 will make the *monoprotonated* second order mechanism competitive, as experimentally observed.

4. Theoretical method

The reaction mechanism has been investigated by the density functional method (DFT),[15] with the recently developed functional M06-2X.[16] All stationary points have been optimized and characterized with the 6-311+G(d,p)[17a–c] basis set and the nature of the critical points checked by vibrational analysis[18] (all data are reported in the Supplementary data). For transition structures (TS), when the inspection of the normal mode related to the imaginary frequency was not sufficient to confidently establish its connection with the initial and final stable species, IRC[19] calculations have been performed. The energy values are then refined through single-point calculations with the basis set 6-311+G(3df,2p)[17d] and combined with the thermal corrections obtained with the smaller basis set to get E+ZPE and free energy values. Solvent effects (water) have been introduced both in geometry optimization and single-point calculations by the Polarized Continuum Method (IEF-PCM).[20]

For a proper description of electronic function and energy estimate relevant to the diradicaloid singlet structures, the spin unrestricted DFT (UDFT) was used.[21] The electronic energy values were then corrected by removing the energy contribution of the triplet electronic function according to an approximate spin projection scheme.[22] All values including the zero point energy, ΔE(0 K) and the thermal and entropy contributions to the free energy, ΔG(273 K) and ΔG(298 K), are discussed and used to estimate, by the Eyring equation, the rate constants. An expectation value of the spin operator S^2 applied to the contaminated singlet indicates, when close to 1, a significant diradical character.[22a] All values are reported in Supplementary data. The natural atomic orbital (NAO) group atomic charges are obtained by the natural population analysis.[23] Calculations were performed by the quantum package Gaussian 09-A.02.[24] Figs. 1, SI-A/F have been obtained with the graphical program Molden.[25]

Acknowledgements

Financial support by local fund by Università di Torino.

Supplementary data

Figures of relevant structures. Tabulated energies (in a.u. and kcal mol^{-1}) and $\langle S^2 \rangle$ values (for diradicaloids only). Cartesian coordinates. Supplementary data related to this article can be found online at doi:10.1016/j.tet.2012.01.014.

References and notes

1. *Advanced Organic Chemistry*; Smith, M. J., March, J., Eds.; John Wiley & Sons: Hoboken, NJ, 2007; pp 1678–1681; Chap. 18–36.
2. See for example (a) Banthorpe, D. V.; Hughes, E. D.; Ingold, C. *J. Chem. Soc.* **1964**, 2864–2901; (b) Shine, H. J. *J. Phys. Org. Chem.* **1989**, *2*, 491–506; (c) Berson, A. *J. Phys. Org. Chem.* **2005**, *18*, 572–577.
3. Osella, S. Master Thesis, 2009. https://wall.rettorato.unito.it/sia/studenti/intesi/Ricerca_tesi_libera/ricerca_tesi_dettaglio.asp?id_upload=8109&cdl_tesi=219&cdl=8&matricola=334454.

4. Ghigo, G.; Osella, S.; Maranzana, A.; Tonachini, G. *Eur. J. Org. Chem.* **2011**, 2326–2333.
5. (a) Dewar, M. J. S. *Nature* **1945**, *156*, 784; (b) Dewar, M. J. S. In *Molecular Rearrangements*; de Mayo, P., Ed.; John Wiley: New York, NY, 1963; Vol. 1, pp 323–343; Chap. 4.A.
6. Yamabe, S.; Nakata, H.; Yamazaki, S. *Org. Biomol. Chem.* **2009**, *7*, 4631–4640.
7. Banthorpe, D. V.; Cooper, A.; Ingold, C. K. *Nature* **1967**, *216*, 232–235.
8. Hammond, J. S.; Shine, H. J. *J. Am. Chem. Soc.* **1950**, *72*, 220–221.
9. Bunton, C. A.; Rubin, R. J. *J. Am. Chem. Soc.* **1976**, *98*, 4236–4246.
10. (a) van Loon, J. P. *Recl. Trav. Chim. Pays-Bas* **1904**, *23*, 62–97; (b) Carlin, R. B. *J. Am. Chem. Soc.* **1945**, *67*, 928–933.
11. Because the accurate theoretical estimation of protonation equilibria is very difficult, we preferred to rely on the ΔG implicit in the experimental equilibrium constants.
12. In the previous work[4] the agreement with the experimental data was not satisfying because we did not take in account the protonation equilibria.
13. (a) Carlin, R. B.; Nelb, R. G.; Odioso, R. C. *J. Am. Chem. Soc.* **1951**, *73*, 1002–1006; (b) Croce, L. J.; Gettler, J. D. *J. Am. Chem. Soc.* **1953**, *75*, 874–879.
14. Rate constants ratios are calculated with the Eyring equation using the computed free energy barriers: $k_d/k_m = \exp(-(\Delta G_d^{\ddagger} - \Delta G_m^{\ddagger})/RT)$.
15. Parr, R. G.; Yang, W. In *Density Functional Theory of Atoms and Molecules*; Oxford University Press: New York, NY, 1989; Chap. 3.
16. (a) Zhao, Y.; Truhlar, D. G. *Theor. Chem. Account* **2008**, *120*, 215–241; (b) Zhao, Y.; Truhlar, D. G. *Acc. Chem. Res.* **2008**, *41*, 157–167; (c) A special issue of PCCP dedicated to the subject Stacking Interactions:Hobza, P., Ed. *Phys. Chem. Chem. Phys.* **2008**, *10*, 2581–2583; (d) Hohenstein, E. G.; Chill, S. T.; Sherrill, C. D. *J. Chem. Theory Comput.* **2008**, *4*, 1996–2000; (e) Peverati, R.; Baldridge, K. K. *J. Chem. Theory Comput.* **2008**, *4*, 2030–2048; (f) Gu, J.; Wang, J.; Leszczynski, J.; Xie, Y.; Schaefer, H. F., III. *Chem. Phys. Lett.* **2008**, *459*, 164–166; (g) Gu, J.; Wang, J.; Leszczynski, J.; Xie, Y.; Schaefer, H. F., III. *Chem. Phys. Lett.* **2009**, *473*, 209–210; (h) Riley, K. E.; Pitonák, M.; Cerný, J.; Hobza, P. *J. Chem. Theory Comput.* **2010**, *6*, 66–80.
17. (a) McLean, A. D.; Chandler, G. S. *J. Chem. Phys.* **1980**, *72*, 5639–5648; (b) Clark, T.; Chandrasekhar, J.; Spitznagel, G. W.; Schleyer, P. v. R. *J. Comput. Chem.* **1983**, *4*, 294–301; (c) Raghavachari, K.; Binkley, J. S.; Seeger, R.; Pople, J. A. *J. Chem. Phys.* **1980**, *72*, 650–654; (d) Frisch, M. J.; Pople, J. A.; Binkley, J. S. *J. Chem. Phys.* **1984**, *80*, 3265–3269.
18. Reaction free energies were computed as outlined, for instance, in: (a) Foresman, J. B.; Frisch, Æ In *Exploring Chemistry with Electronic Structure Methods*; Gaussian: Pittsburgh, PA (USA), 1996; pp 166–168; (b) McQuarrie, D. A. *Statistical Thermodynamics*; Harper and Row: New York, NY, 1973.
19. (a) Gonzalez, C.; Schlegel, H. B. *J. Chem. Phys.* **1989**, *90*, 2154–2161; (b) Gonzalez, C.; Schlegel, H. B. *J. Phys. Chem.* **1990**, *94*, 5523–5527 and references therein.
20. (a) Barone, V.; Cossi, M. *J. Phys. Chem. A* **1998**, *102*, 1995–2001; (b) Cossi, M.; Rega, N.; Scalmani, G.; Barone, V. *J. Chem. Phys.* **2001**, *114*, 5691–5701; (c) Cancès, M. T.; Mennucci, B.; Tomasi, J. *J. Chem. Phys.* **1997**, *107*, 3032–3041; (d) Cossi, M.; Barone, V.; Mennucci, B.; Tomasi, J. *Chem. Phys. Lett.* **1998**, *286*, 253–260; (e) Mennucci, B.; Tomasi, J. *J. Chem. Phys.* **1997**, *106*, 5151–5158.
21. For a review of computational methods that are appropriate for different types of open-shell molecules see: Bally, T.; Borden, W. T. In *Reviews in Computational Chemistry*; Lipowitz, K. B., Boyd, D. B., Eds.; Wiley: New York, NY, 1999.
22. (a) Yamaguchi, K.; Takahara, Y.; Fueno, T.; Houk, K. N. *Theor. Chim. Acta* **1988**, *73*, 337–364; (b) Yamaguchi, K.; Jensen, F.; Dorigo, A.; Houk, K. N. *Chem. Phys. Lett.* **1988**, *149*, 537–542; (c) Yamanaka, S.; Kawakami, T.; Nagao, K.; Yamaguchi, K. *Chem. Phys. Lett.* **1994**, *231*, 25–33; (d) Goldstein, E.; Beno, B.; Houk, K. N. *J. Am. Chem. Soc.* **1995**, *118*, 6036–6043; (e) Isobe, H.; Takano, Y.; Kitagawa, Y.; Kawakami, T.; Yamanaka, S.; Yamaguchi, K.; Houk, K. N. *J. Phys. Chem. A* **2003**, *107*, 682–694; (f) Kitagawa, Y.; Saito, T.; Nakanishi, Y.; Kataoka, Y.; Matsui, T.; Kawakami, T.; Okumura, M.; Yamaguchi, K. *J. Phys. Chem. A* **2009**, *113*, 15041–15046.
23. (a) Foster, J. P.; Weinhold, F. *J. Am. Chem. Soc.* **1980**, *102*, 7211–7218; (b) Reed, A. E.; Weinhold, F. *J. Chem. Phys.* **1983**, *78*, 4066–4073; (c) Reed, A. E.; Weinstock, R. B.; Weinhold, F. *J. Chem. Phys.* **1985**, *83*, 735–746.
24. Frisch, M. J.; Trucks, G. W.; Schlegel, H. B.; Scuseria, G. E.; Robb, M. A.; Cheeseman, J. R.; Scalmani, G.; Barone, V.; Mennucci, B.; Petersson, G. A.; Nakatsuji, H.; Caricato, M.; Li, X.; Hratchian, H. P.; Izmaylov, A. F.; Bloino, J.; Zheng, G.; Sonnenberg, J. L.; Hada, M.; Ehara, M.; Toyota, K.; Fukuda, R.; Hasegawa, J.; Ishida, M.; Nakajima, T.; Honda, Y.; Kitao, O.; Nakai, H.; Vreven, T.; Montgomery, J. A., Jr.; Peralta, J. E.; Ogliaro, F.; Bearpark, M.; Heyd, J. J.; Brothers, E.; Kudin, K. N.; Staroverov, V. N.; Kobayashi, R.; Normand, J.; Raghavachari, K.; Rendell, A.; Burant, J. C.; Iyengar, S. S.; Tomasi, J.; Cossi, M.; Rega, N.; Millam, N. J.; Klene, M.; Knox, J. E.; Cross, J. B.; Bakken, V.; Adamo, C.; Jaramillo, J.; Gomperts, R.; Stratmann, R. E.; Yazyev, O.; Austin, A. J.; Cammi, R.; Pomelli, C.; Ochterski, J. W.; Martin, R. L.; Morokuma, K.; Zakrzewski, V. G.; Voth, G. A.; Salvador, P.; Dannenberg, J. J.; Dapprich, S.; Daniels, A. D.; Farkas, Ö; Foresman, J. B.; Ortiz, J. V.; Cioslowski, J.; Fox, D. J. *Gaussian 09, Revision A.02*; Gaussian: Wallingford CT, 2009.
25. Molden: Schaftenaar, G.; Noordik, J. H. *J. Comput.-Aided Mol. Des.* **2000**, *14*, 123–134.